Magnitude and Origin of the Difference in Vibrational Entropy between Ordered and Disordered Fe_3Al

L. Anthony, L. J. Nagel, J. K. Okamoto, and B. Fultz
California Institute of Technology, 138-78 Pasadena, California 91125
(Received 1 August 1994)

The difference in vibrational entropy between chemically disordered and DO_3-ordered Fe_3Al was measured by calorimetry to be $(0.10 \pm 0.03)\,k_B$/atom at high temperatures, with the ordered alloy having the lower vibrational entropy. Analysis of the vibrational modes of the ordered and disordered alloys with a Born–von Kármán model showed that the lower vibrational entropy of the ordered alloy originates from high-frequency optical modes involving large-amplitude vibrations of the aluminum-rich sublattice.

PACS numbers: 81.30.Hd, 63.70.+h, 64.70.Kb

The present Letter concerns the entropy change of a chemical disorder-order transition, where a crystalline binary alloy changes from a random solid solution to an ordered intermetallic compound. An important and well-understood change occurs in the "configurational entropy," which enumerates the number of ways that atoms can be arranged on the crystal lattice, given an overall state of order for the alloy [1–3]. Heat is evolved or absorbed as the atoms change their configuration on the lattice, because these configurational changes alter the chemical bonding in the alloy.

Heat can also be absorbed directly into the vibrational modes of the crystal, however, without moving the atoms between lattice sites. It seems reasonable that alloys in different (but constant) configurational states could differ in their "vibrational entropy." In spite of some general theoretical work [4–9], and some experimental data on martensitic transformations [10,11], vibrational entropy has attracted little attention. Recently, however, the difference in vibrational entropy between ordered and disordered Ni_3Al was measured and found to be about $0.3k_B$/atom [12]. This is of comparable magnitude to the difference in configurational entropy ($0.56k_B$/atom), so vibrational entropy can be thermodynamically important. Here we report new calorimetric measurements for the difference in vibrational entropy between ordered and disordered Fe_3Al. While this measured difference of $(0.10 \pm 0.03)k_B$/atom is not as large as for Ni_3Al, Fe_3Al offers an important advantage for understanding the origin of differences in vibrational entropy. Phonon dispersion relations from inelastic neutron scattering have been used to obtain Born-von Kármán force constants for both the ordered and disordered states of Fe_3Al [13–15]. From these force constants we obtained one-phonon densities of states (DOS) and used them to calculate the lattice heat capacities and the vibrational entropies. We show that the smaller vibrational entropy of the ordered Fe_3Al is due largely to the development of high-frequency optical modes involving large-amplitude vibrations of the aluminum-rich sublattice.

An alloy of Fe-25 at. % Al was prepared from materials of 99.99% purity by arcmelting under an argon atmosphere. The composition and homogeneity of this alloy had been characterized thoroughly in previous studies of chemical ordering transformations [16,17]. For the present work, samples of chemically disordered Fe_3Al were prepared by filing. X-ray powder diffractometry showed no superlattice diffractions from the as-filed powders. Mössbauer spectrometry, which is primarily sensitive to short-range order [18], showed that these filed powders were largely disordered bcc solid solutions. A state of DO_3 chemical order was obtained in the samples by annealing them in evacuated borosilicate glass ampoules at 480 °C for 1 h. Strong x-ray superlattice diffractions were measured from the annealed powders, indicating a long-range order parameter of close to unity. X-ray diffraction line broadening measurements, checked with dark field imaging in a transmission electron microscope, showed that the grain sizes of the as-filed powders were 13 nm, increasing to 20 nm after annealing.

Low-temperature heat capacity measurements employed a Perkin Elmer DSC–4 differential scanning calorimeter (DSC) that had been modified by installing its sample head in a liquid helium Dewar. Masses (about 40 mg) of the disordered and ordered alloys were matched to 10 μg accuracies and placed in the two sample pans of the DSC. Heat capacity measurements comprised pairs of runs, with the two samples interchanged in their sample pans between runs. The difference in heat capacities of the two samples was obtained from the difference of these two sets of runs. To test reproducibility, we obtained 5 matched pairs of runs with liquid nitrogen and 2 matched pairs with liquid helium as the cryogen. To counteract instrumental drift, runs comprised three pairs of scans over small temperature intervals of 30 K, which typically overlapped by 10 K. All scans were at 40 K min^{-1}. Additional calibration runs were performed with ordered Fe_3Al against a NIST sapphire standard.

 0031-9007/94/73(22)/3034(4)$06.00

The difference in variational entropy, $\Delta S_{\rm vib} = S^D - S^O$, between disordered ($D$) and ordered ($O$) samples was obtained from the measured difference in heat capacity at constant pressure, $\Delta C_p \equiv C_p^D - C_p^O$:

$$\Delta S_{\rm vib}(T_1, T_2) = \int_{T_1}^{T_2} \frac{\Delta C_p}{T}\, dT . \qquad (1)$$

Ideally, $T_1 = 0$ K and T_2 is the temperature of interest, such as the critical temperature of the order-disorder transition. The range of our experimental data was from 80 to 343 K. The upper limit of this range was chosen to suppress changes in the configurational entropy. Diffusional atom movements in Fe_3Al are negligible at these low temperatures [16,17]. Were diffusion to occur, it would be largest at the highest temperatures of measurement, giving a strongly decreasing ΔC_p. Changes in the state of order could also modify the reproducibility of the three pairs of scans taken in each temperature interval or the reproducibility of the different runs with the same samples. None of these problems were found, so we are confident that the measurements provided differences in the vibrational heat capacity, unencumbered by changes in the configurational entropy with its evolution of heat.

Averaged results from the calorimetry measurements are presented in Fig. 1. The sign of the data is positive, showing that the disordered state of Fe_3Al has the larger heat capacity. The data of Fig. 1 were fitted to a difference of two Debye functions with $\theta^D_{\rm Debye} = 484$ K and $\theta^D_{\rm Debye} = 500$ K to correct the integral of Eq. (1) for the missing low- and high-temperature contributions. After correction, we obtain a difference in vibrational entropy $\Delta S_{\rm vib}$ of $(0.10 \pm 0.03) k_B$/atom at high temperatures. While smaller than the maximum possible configurational entropy of mixing ($0.56 k_B$/atom for the Fe_3Al stoichiometry), $\Delta S_{\rm vib}$ is not negligible.

Van Dijk [13] and Robertson [14,15] have used inelastic neutron scattering to measure phonon dispersion curves along high-symmetry directions in ordered and disordered Fe_3Al. Using Robertson's force constants up to fifth neighbors (columns 1 and 3 of Table 4 in [15]), we calculated the phonon DOS for disordered and DO_3-ordered Fe_3Al. In these calculations the disordered state was represented as a bcc lattice with a basis of 1 atom having an average mass of the Fe and Al atoms, and the bcc-based DO_3-ordered structure was represented as an fcc lattice with a 4-atom basis. The phonon dispersion relations for high-symmetry directions were reproduced and were in excellent agreement with those presented by Robertson [15]. The dynamical matrix $D(\mathbf{q})$ (3×3 for the disordered state, 12×12 for the ordered state) was diagonalized for approximately 5 million values of $\mathbf{q}$ distributed evenly over the irreducible portion of the first Brillouin zone ($\frac{1}{48}$ of the total zone) of the disordered alloy and approximately 10 million values for the ordered alloy. The resulting phonon DOS curves for the disordered and ordered alloys, $g^D(\nu)$ and $g^O(\nu)$, are presented in Fig. 2. The actual phonon DOS of the disordered alloy would have its sharp features broadened significantly, but this will not affect qualitatively the arguments that follow.

These DOS curves were then used to calculate lattice heat capacities. Each normal mode was given a phonon occupation set by Bose-Einstein statistics. The heat capacity of the disordered and ordered materials is the heat capacity per mode integrated over the corresponding phonon DOS. The difference in heat capacity,

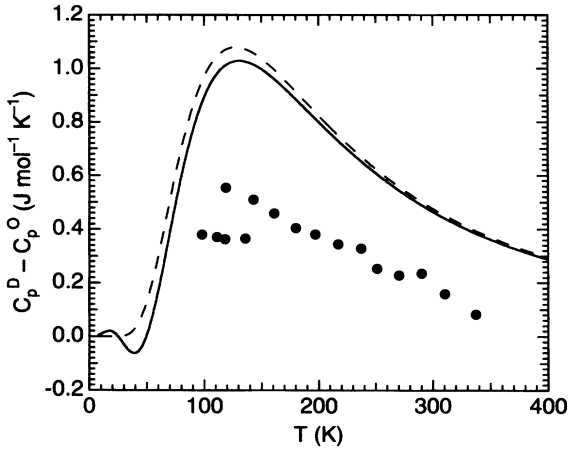

FIG. 1. Points are measured differential heat capacity of ordered and disordered samples of Fe_3Al, $\Delta C_p = C_p^D - C_p^O$, as a function of T. Curves were calculated using Eq. (2), with the solid curve using the DOS from the main part of Fig. 2, and the broken curve using the DOS from the inset of Fig. 2.

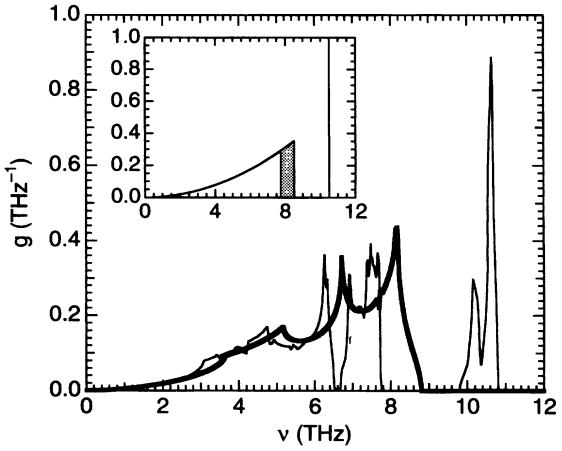

FIG. 2. Phonon DOS curves for ordered (thin curve) and disordered (thick curve) Fe_3Al, calculated using force constants from Robertson [15]. Inset: simplified phonon DOS curves, disordered Fe_3Al curves comprise unshaded and shaded parts, ordered Fe_3Al curves comprise unshaded part and delta function at 10.5 THz.

$\Delta C_V(T) = C_V^D - C_V^O$, is

$$\Delta C_V(T) = 3Nk_B \int_0^\infty (g^D(\nu) - g^O(\nu)) \times \left(\frac{h\nu}{k_BT}\right)^2 \frac{\exp\frac{h\nu}{k_BT}}{\left(\exp\left(\frac{h\nu}{k_BT}\right) - 1\right)^2} d\nu. \quad (2)$$

The calculation from Eq. (2) is presented as a solid curve in Fig. 1. There is qualitative agreement between the calculated and measured $\Delta C_V(T)$. The disparity could originate with several sources, including the different composition of Robertson's disordered sample [15]. Substituting Eq. (2) for $\Delta C_V(T)$ into Eq. (1) and integrating, we obtain a $\Delta S_{\text{vib}} = 0.186 k_B$/atom in the high-temperature limit.

Figure 3 presents the phonon partial DOS for the three nonequivalent crystallographic sites [4(a), 4(b), and 8(c) in Wyckoff notation] in the DO_3 ordered structure [19]. These were obtained by weighting the phonon DOS by the factor $|\sigma_{\mathbf{d}}^{\gamma}(\mathbf{q})|^2$, where $\sigma_{\mathbf{d}}^{\gamma}(\mathbf{q})$ is the normalized (polarization) eigenvector for the basis atom at position $\mathbf{d}$ in the unit cell, for a given phonon branch γ of wave vector $\mathbf{q}$. From Fig. 3 it is apparent that the high-frequency modes around 10.5 THz originate primarily from the vibrations of the 4(a) Al atoms and, to a lesser extent, from the surrounding 8(c) Fe atoms. This can be understood as being due to large-amplitude high-frequency vibrations of low-mass Al atoms in a cubical cage of eight surrounding 8(c) Fe atoms. The 8(c) Fe atoms vibrate in response to the Al atoms at the same frequency but, being more massive, do so with smaller amplitudes (see Fig. 3). Similarly, the intermediate-frequency modes between about 7 and 8 THz are due mostly to the vibrations of the 4(b) Fe atoms in their cage of nearest-neighbor 8(c) Fe atoms. Most of the thermal kinetic energy of the Al atoms is associated with the high-frequency modes around 10.5 THz in the ordered structure. Since the Al atoms are the minority species in Fe_3Al, the Al atoms undergo the largest change in local chemical environment upon ordering. We therefore expect these high-frequency modes at 10.5 THz to be strongly sensitive to the state of chemical order in the alloy.

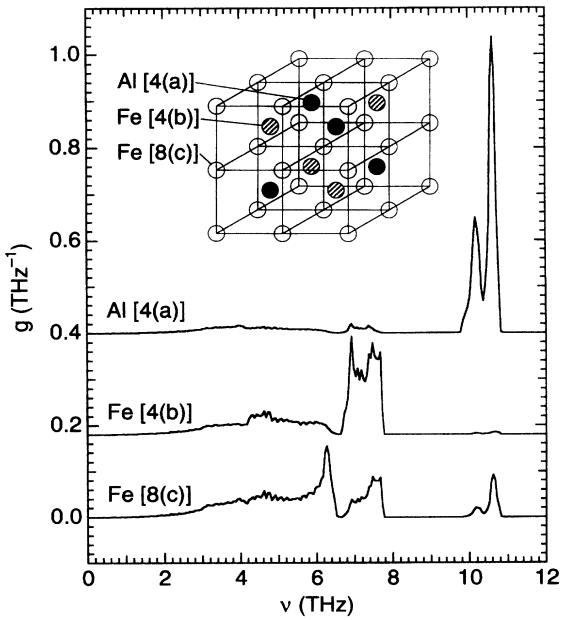

FIG. 3. Phonon partial DOS for the three nonequivalent crystallographic sites in the DO_3 structure, shown in inset.

The reason that ordered Fe_3Al has a lower vibrational entropy than disordered Fe_3Al is that there is a low phonon occupation of the high-frequency modes associated with the formation of an Al-rich sublattice. The lattice heat capacity and vibrational entropy are not sensitive to fine details of the phonon DOS, so we can provide a simplified model in the inset in Fig. 2. The model uses a Debye model for the disordered alloy with $\nu_{\text{Debye}} = 8.5$ THz. For the ordered alloy, we deleted the top $\frac{1}{4}$ of the modes in the Debye model (from $(\frac{3}{4})^{1/3}\nu_{\text{Debye}}$ to ν_{Debye} of the disordered alloy) and placed them in a single high-frequency Einstein-like distribution at $\nu_{\text{Einstein}} = 10.5$ THz. The $\Delta C_V(T)$ for this model, calculated with Eq. (2), is presented as a dashed curve in Fig. 1, and the high-temperature limit of its $\Delta S_{\text{vib}}(T)$ was $0.185 k_B$/atom.

Other ordered alloys also exhibit such high-frequency modes which seem to originate with stiffly bonded, low-mass atoms [20–22]. We expect these ordered alloys to have a lower vibrational entropy than their disordered counterparts, but no experimental data are available on the phonon DOS of these alloys in disordered states. We know of one other alloy, Cu_3Au, for which inelastic neutron scattering data were obtained for both ordered and disordered states [23]. We used the published force constants for Cu_3Au to calculate a ΔS_{vib} of $0.232 k_B$/atom in the high-temperature limit. (Recent calculations of Cleri and Rosato on Cu_3Au [24] give $0.12 k_B$/atom.) This disagrees with the ΔS_{vib} of $0.075 k_B$/atom implied by a previous study using calorimetry at temperatures below 4.2 K [25], but such low temperature measurements would be insensitive to high-frequency phonon modes. We also note that the difference in electronic heat capacity [25] provides a thermodynamically negligible contribution to the entropy.

We acknowledge the help and interest of Dr. C. C. Ahn and conversations with G. Ackland, G. D. Garulsky, and G. Ceder. This work was supported by the U.S. Department of Energy under Contract No. DE-FG03-86ER45270.

[1] See, for example, F. Ducastelle, *Order and Phase Stability in Alloys* (North-Holland, Amsterdam, 1991).

[2] L. Onsager, Phys. Rev. **65**, 117 (1944).
[3] R. Kikuchi, Phys. Rev. **81**, 1988 (1951).
[4] C. Booth and J. S. Rowlinson, Trans. Faraday Society, **51**, 463 (1955).
[5] P. J. Wojtowciz and J. G. Kirkwood, J. Chem. Phys. **33**, 1299 (1960).
[6] H. Bakker, Philos. Mag. A **45**, 213 (1982).
[7] J. A. D. Matthew, R. E. Jones, and V. M. Dwyer, J. Phys. F **13**, 581 (1983).
[8] H. Bakker and C. Tuijn, J. Phys. C **19**, 5585 (1986).
[9] G. D. Garbulsky and G. Ceder, Phys. Rev. B **49**, 6327 (1994).
[10] J. W. Cahn, Prog. Mater. Sci. **36**, 149 (1992).
[11] A. Planes, L. Manosa, D. Rios-Jara, and J. Ortin, Phys. Rev. B **45**, 7633 (1992).
[12] L. Anthony, J. K. Okamoto, and B. Fultz, Phys. Rev. Lett. **70**, 1128 (1993).
[13] C. Van Dijk, Phys. Lett. **A 34**, 255 (1970).
[14] I. M. Robertson, Solid State Commun. **53**, 901 (1985).
[15] I. M. Robertson, J. Phys. Condens. Matter **3**, 8181 (1991).
[16] Z. Q. Gao and B. Fultz, Philos. Mag. B **67**, 787 (1993).
[17] B. Fultz and Z. Q. Gao, Nucl. Instrum. Methods Phys. Res. Sect. B **76**, 115 (1993).
[18] B. Fultz, in *Mössbauer Spectroscopy Applied to Magnetism and Materials Science,* edited by G. J. Long and F. Grandjean (Plenum Press, New York, 1993), Chap. 1, pp. 1–31.
[19] P. Villars and L. D. Calvert, *Pearson's Handbook of Crystallographic Data for Intermetallic Phases,* 2nd ed. (ASTM International, Newbury, Ohio, 1991).
[20] C. Stassis, F. X. Kayser, C.- K. Loong, and D. Arch, Phys. Rev. B **24**, 3048 (1981).
[21] M. Mostoller, R. M. Nicklow, D. M. Zehner, S.-C. Lui, J. M. Mundenar, and E. W. Plummer, Phys. Rev. B **40**, 2856 (1989).
[22] Y. Noda and Y. Endoh, J. Phys. Soc. Jpn. **12**, 4225 (1988).
[23] S. Katano, M. Iizumi, and Y. Noda, J. Phys. F **18**, 2195 (1988).
[24] F. Cleri and V. Rosato, Philos. Mag. Lett. **67**, 369 (1993).
[25] J. Rayne, Phys. Rev. **108**, 649 (1957).

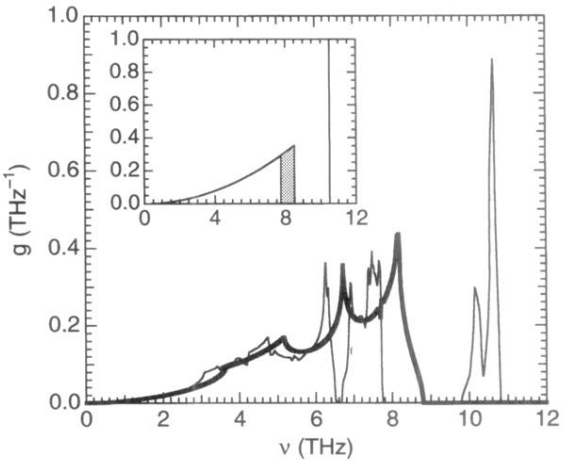

FIG. 2. Phonon DOS curves for ordered (thin curve) and disordered (thick curve) Fe_3Al, calculated using force constants from Robertson [15]. Inset: simplified phonon DOS curves, disordered Fe_3Al curves comprise unshaded and shaded parts, ordered Fe_3Al curves comprise unshaded part and delta function at 10.5 THz.